California Geological Survey
Fault Evaluation Report FER 261

The West Tahoe Fault

in the Emerald Bay and Echo Lake Quadrangles
El Dorado County, California

by
Gordon Seitz
Engineering Geologist

Introduction

The Tahoe Basin is located at the boundary between the Sierra Nevada microplate and the Great Basin (Unruh et al., 2003; Dingler et al., 2009; Schweickert et al., 2004). This region is part of the Walker Lane, an approximately 100 km wide and 600+ km long northwest-southeast trending zone of relatively dense active faulting. The Walker Lane includes many normal and strike-slip faults that accommodate part of the right-lateral shear between the North American and Pacific plates; more specifically the Sierra Nevada microplate and the Great Basin (Unruh et al., 2003; Bormann, 2013).

The Tahoe Basin was first unambiguously recognized as resulting from active extensional faulting by several offshore geophysical surveys of Lake Tahoe (Hyne et al., 1972; Gardner et al., 2000; Kent et al., 2005). These surveys revealed well-defined fault scarps on the otherwise flat lake bottom and vertical offsets in Holocene-age lake sediments.

The central portion and majority of the Tahoe Basin is covered by Lake Tahoe. This report covers the southwest portion of the basin, which has a flatter shelf that extends from the lake to the highlands lying to the west (Fig. 2, Plates 1, 2). This shelf increases in width, from about 1 km north of Emerald Bay south 12 km to near Highway 50. In general these flatter portions that abut the lake are underlain by glacial and fluvial deposits and landforms. North of Emerald Bay this bedrock shelf is elevated, consistent with its position on the uplifted footwall block of the offshore West Tahoe Fault.

The West Tahoe Fault has a mapped length of 45 km (Fig. 1). It is the range bounding, east dipping normal fault along the west margin of the basin. South of Emerald Bay the West Tahoe Fault extends onshore as two parallel strands. In the lake, the fault has clearly defined scarps that offset submarine fans, lake-bottom sediments, and the McKinney Bay slide deposits (Seitz, 2014, Hyne et al, 1972; Gardner et al, 2000; Kent et al, 2005; Dingler et al. 2009).

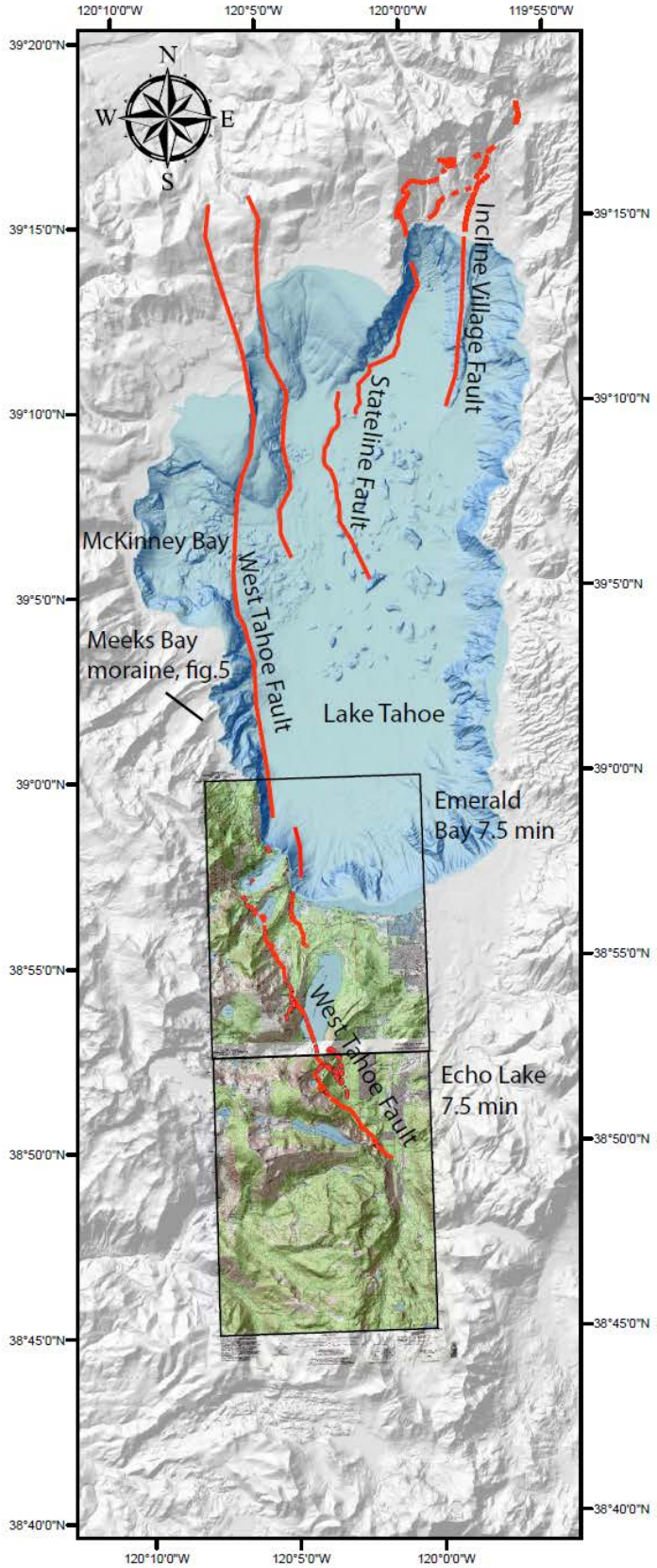

Figure 1. Tahoe Basin Fault Map with Quadrangle Maps Evaluated. .
Three active faults cross the Tahoe Basin as shown with red lines. The focus of this report is on the southern portion of the West Tahoe fault where it extends onshore. High resolution multibeam bathymetry and Lidar topography have been instrumental in revealing the exact locations of active faults. The onshore image is a hill shade, the offshore is a slope shade.

Kent et al. (2005) and Dingler et al. (2009) estimate the slip rate on the West Tahoe Fault to be 0.6-1.0 mm year, based on displacement of a submerged shoreline across the basin and the fault being the only active fault mapped in the southern Tahoe Basin. An offshore sediment core was used to date the submerged shoreline. This slip rate is the highest of any fault in the Tahoe Basin.

The purpose of this report is to assess the location and activity of the onshore portions of the West Tahoe Fault within the Emerald Bay and Echo Lake 7.5 minute quadrangle maps (Fig.1). These two 7.5 min quadrangle topographic maps cover the southernmost extent of the West Tahoe Fault. In this area, the West Tahoe Fault is expressed as a sharp fault scarp, primarily in glacial deposits of Tahoe and Tioga age. Other mapped faults in the area were also evaluated. This study and a recent basin-wide study by Kent et al. (2015) use high-resolution Lidar data to evaluate this portion of the West Tahoe Fault. A previous effort by Howle et al. (2012) used older, lower-resolution, and less extensive Lidar data. The differences will be discussed in the fault section portions of this report. Faults determined to be sufficiently active (Holocene-age, ~11 ka) and well-defined are zoned by the State Geologist as mandated by the Alquist-Priolo Earthquake Fault Zoning (AP) Act of 1972 (Bryant and Hart, 2007).

Geologic Setting

The Tahoe Basin is bounded by the Sierra Nevada on the west and the Carson Range to the east. These ranges are predominately composed of Cretaceous-age granitic rocks mantled by Tertiary-age volcanic rocks (Saucedo, 2005). West of Fallen Leaf Lake, the granitic rocks surround older metamorphic roof pendants. The Tahoe Basin is the westernmost basin of the Basin and Range extensional province. The basin is an asymmetric half graben (Dingler et al., 2009) and has been active for at least the past 3 m.y. (Surpless et al., 2002; Faulds et al., 2005).

Three active, north-striking normal faults in the Tahoe Basin have been defined by on and offshore studies (Kent et al., 2005; Dingler et al., 2009; Kent et al., 2015). Total extension across all three basin forming faults estimated from geologic separations is 0.84 mm/yr (0.53-1.15) (Dingler et al., 2009), or more than 30% of east-west extension observed along Sierra Frontal faults through geodetic measurements spanning the Walker Lane (Hammond and Thatcher, 2004).

Glacial Deposits and Geomorphology

Most of the area crossed by the on-land section of the West Tahoe Fault is underlain by glacial deposits of Pleistocene age. Two clearly recognized late Pleistocene-age glaciations are referred to as the Tahoe and Tioga (Blackwelder, 1931; Birkeland, 1961; 1964; McCaughey, 2003). In general, the two glacial maxima are recognized as the highest lateral moraines that extend from the margins of glacial valleys at the range front towards the shoreline (fig 3). The moraine crests are about 100 to 200 m higher than the surrounding landscape. The older Tahoe-age maximum moraine generally lies in a slightly higher landscape position than the younger Tioga-age moraines. The Tioga-age moraines parallel the Tahoe moraines, and often truncate the lower portions of them. Thus the entire set of Tioga moraines is generally much more complete. For

example at Fallen Leaf Lake a remarkable series of 22 Tioga-age recessional moraines is preserved (Fig. 2, 3, Plates 1, 2).

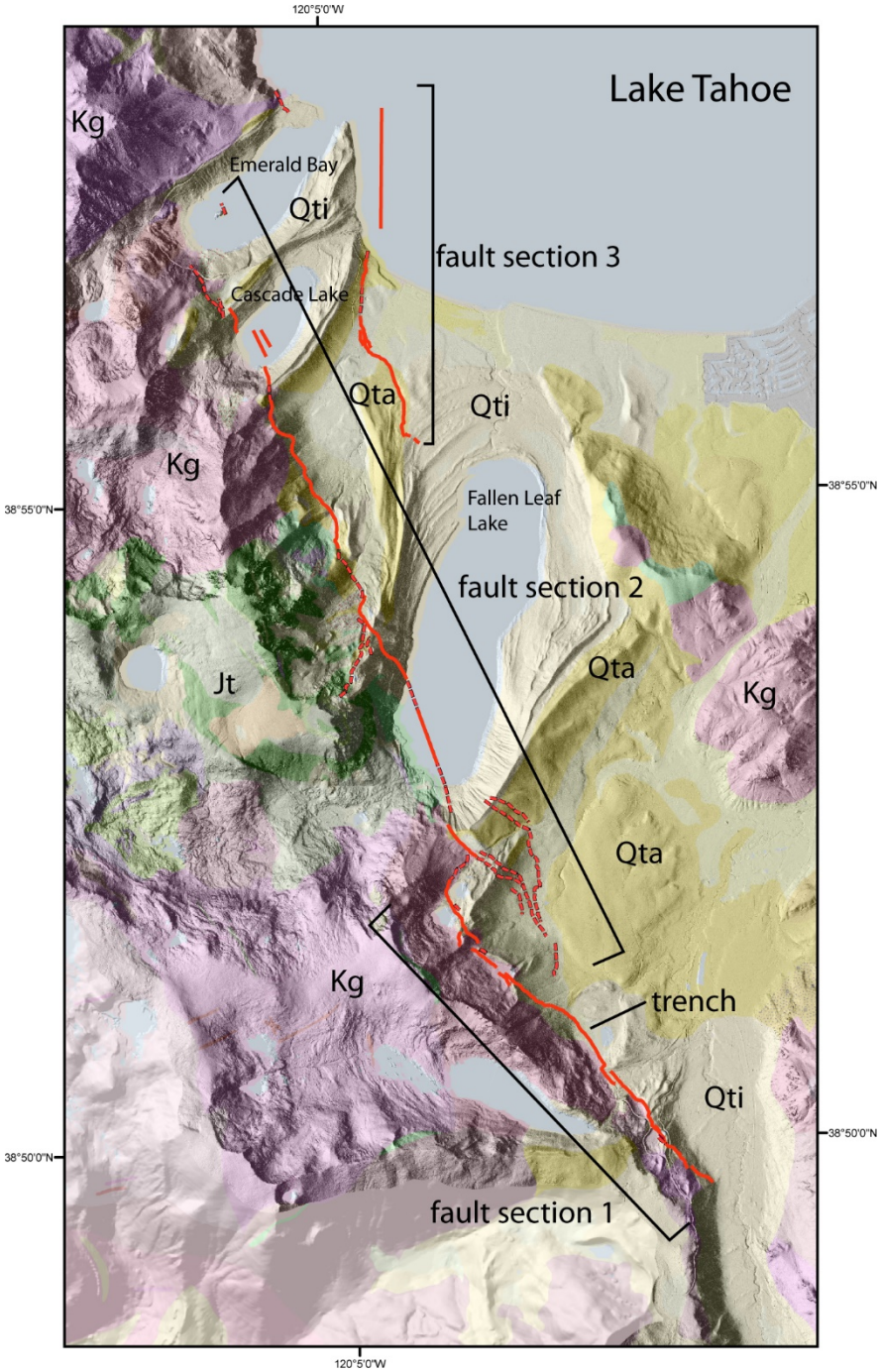

Figure 2. West Tahoe Fault Map. This map shows the southern portion of the West Tahoe fault where it extends onshore south of Emerald Bay. The fault has been divided into fault sections based on trend and continuity. Geological units are indicated from youngest to oldest:
Jt-Jurrasic Metamorphics,
Kg-Cretaceous Granitics,
Qta-Tahoe-age Glacial Deposits,
Qti- Tioga-age Glacial Deposits.
The location of a fault investigation location with a trench is shown in Section 1. This is the only onshore location where the faulted deposits are dated directly.

Glacial Chronology

Most of the age estimates for glacial deposits in the Tahoe Basin rely on correlations with numerically dated moraines elsewhere along the Sierra Nevada. These regional correlations are fraught with uncertainty and hence we focus here on several age determinations from the Tahoe Basin that can be correlated directly to faulted deposits in the evaluated area.

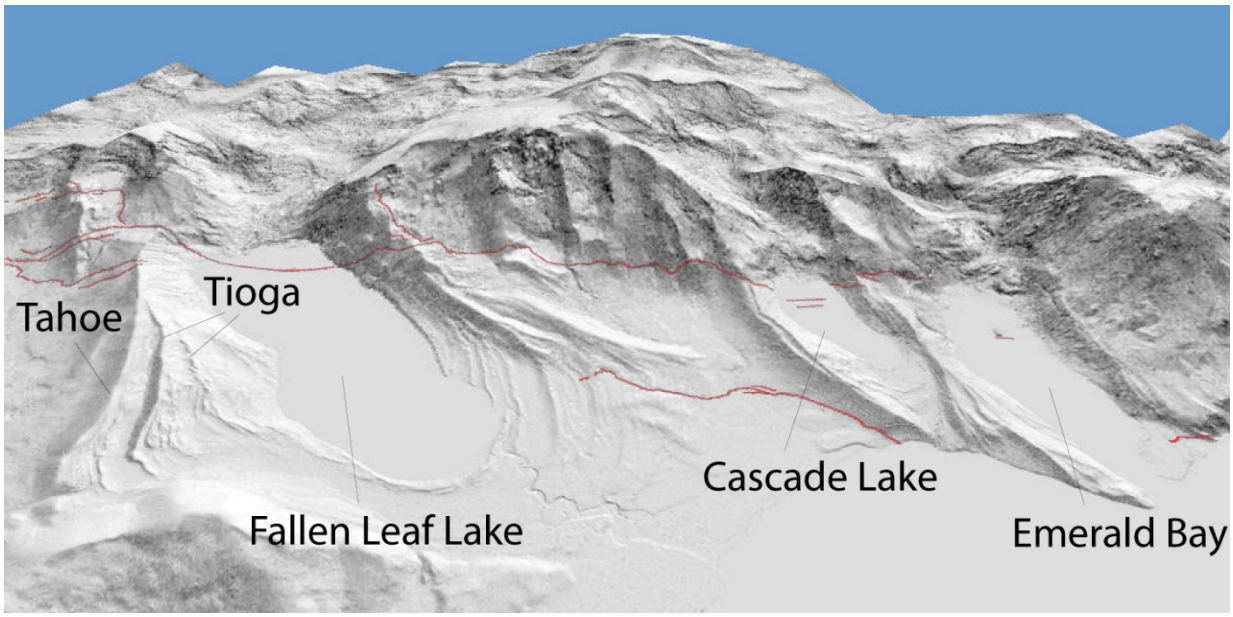

Figure 3. Glacial Moraines Along the West Shore of Lake Tahoe. The paired glacial moraines which extend the highland glacial valleys from the range front towards the Lake Tahoe, but also formed Fallen Leaf Lake , Cascade Lake and Emerald Bay. The older flatter crested Tahoe-age (70 ka) moraine along Fallen Leaf Lake and a sharper crested Tioga-age (20 ka) maximum moraine are shown. The West Tahoe fault is shown with red lines.

On the west side of Lake Tahoe near Meeks Bay, north of Emerald Bay (Fig. 4), the two highest moraine crests were dated using cosmogenic nuclide surface exposure analyses for ^{26}AL and ^{10}Be (Howle et al., 2005; 2012). The well preserved moraines at Meeks Bay consist of granitic till. Several samples were taken from the tops of boulders. The highest Tahoe-age moraine was dated at 69.2±4.8 ka, and the Tioga-age moraine was dated at 20.8±1.4 ka. These dates are currently the only direct dates of these moraines in the Tahoe Basin, and appear reasonable compared to other Sierra Nevada localities. A single optically stimulated luminescence (OSL) date of 73±8.7 ka consistent with the above Tahoe-age moraine crest was reported by Howle et al. (2012, as a pers. com. from Berger, G.W. at DRI) for a sample collected below the glacial till in lacustrine silt deposits at Taylor Creek.

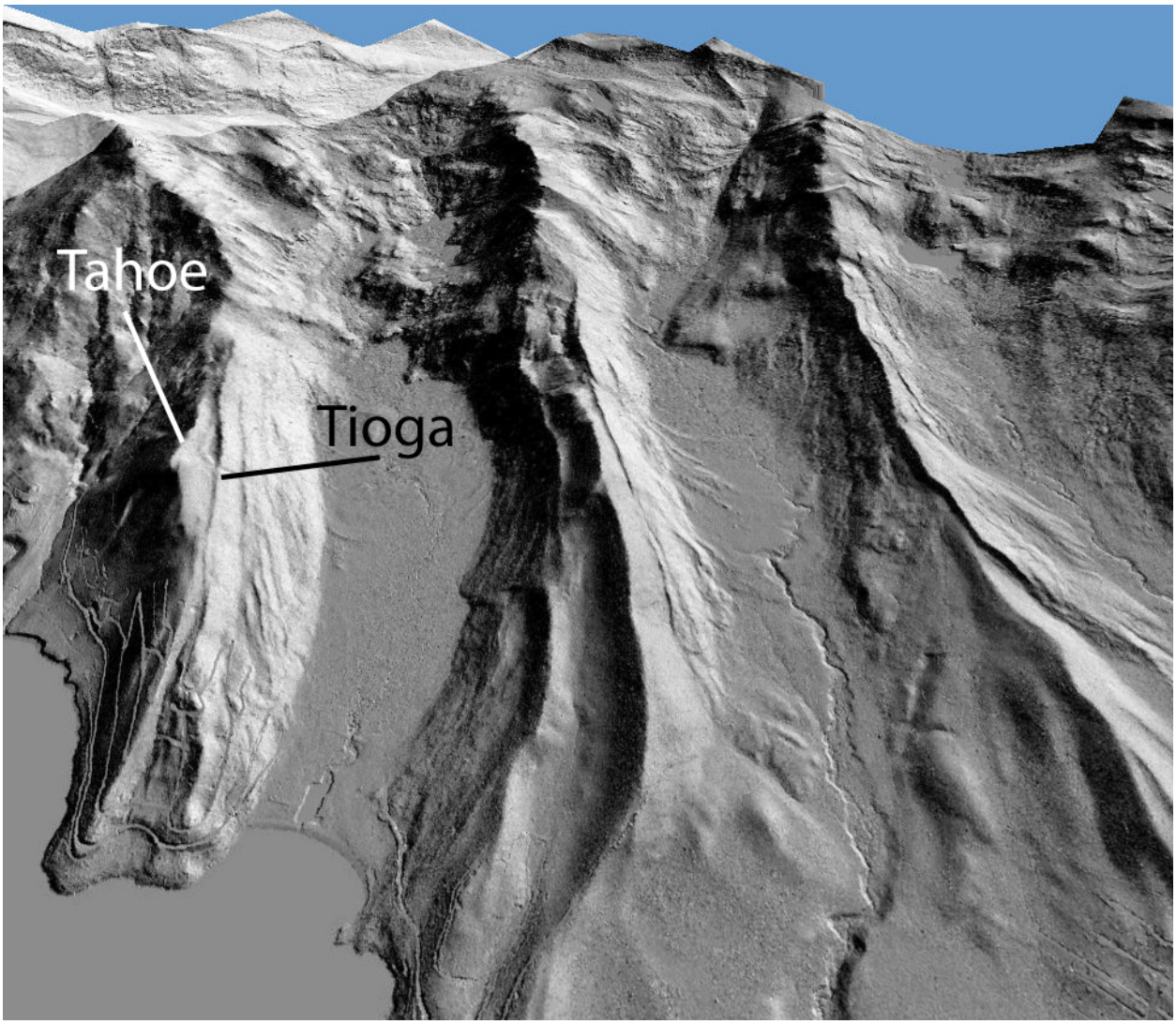

Figure 4. **Meeks Bay Moraines. The locations of samples age dated by cosmogenic surface exposure techniques are indicated (Howle et al., 2005; 2012).**

Relative dating of the highest moraines throughout the basin is possible because the two-fold glacial history has resulted in a relatively simple and distinct set of two morainal complexes of Tioga and Tahoe age. Even prior to the availability of high resolution topography, it was recognized that the older Tahoe-age moraines exhibited rounder, flatter, and wider crests with more deeply weathered boulders (Blackwelder, 1931; Birkeland, 1961; 1964; McCaughey, 2003). Specifically for the southwest Tahoe Basin, McCaughey (2003) quantified the different weathering related field parameters that differentiate the Tahoe- and Tioga-age glacial deposits. He was able to show that the moraine crests flatten significantly over time, allowing the distinction between the Tahoe-age moraines at 70 ka and the Tioga-age moraines at 20 ka. This

difference in moraine crest geomorphology can now be used as a relative dating method, using the dated Meeks Bay moraines as calibration (Fig. 3, 4).

Fault Mapping

On and offshore studies in the Tahoe Basin (Seitz and Kent, 2004; Kent et. al, 2005; Dingler et al., 2009; Brothers et al., 2009; Smith et al., 2013; Maloney et al, 2014; Kent et al, 2015), have revealed three active normal faults that are significant seismic sources (Fig. 1). Using high-resolution seismic Compressed High Intensity Radar Pulse (CHIRP) profiles, combined with age dating of sediment cores using radiocarbon (C-14) and OSL techniques, have allowed estimates for slip rates for the West Tahoe Fault (WTF), Stateline Fault (SF) and Incline Village Fault (IVF). Offset submerged paleolake terraces and a catastrophic slide debris deposit provide markers for vertical slip rates of 0.6 mm/yr (0.44-1.1), 0.45 mm/yr (0.35-0.6) and 0.2 mm/yr (0.12-0.3) on the WTF, SF and IVF, respectively (Kent et al., 2005; Dingler et al., 2009). Total extension across all three basin forming faults is estimated to be 0.84 mm/yr (0.53-1.15).

The WTF has a mapped length of 45 km (Fig. 1), and is the range bounding, east dipping normal fault along the west margin of the basin, and is largely located along the western base of Lake Tahoe at a water depth of 400-500 m. In the lake, the fault has clearly defined scarps that offset submarine fans, lake-bottom sediments, and the McKinney Bay slide deposits (Hyne et al, 1972; Gardner et al, 2000; Kent et al, 2005; Dingler et al. 2009). Recent work analyzing sediment cores from the lake bottom has clearly shown that earthquakes on the local faults trigger landslides in the lake (Smith et al., 2013). These triggered landslides in turn stir up the lake sediments which form distinct and wide-spread sediment deposits termed turbidites. Sediment cores have revealed a long-term record of strong earthquake ground shaking frequency, with between 14 to 17 events recognized in the past 12 thousand years.

The most recent offshore studies conducted in Fallen Leaf Lake, Cascade Lake and Lake Tahoe (Brothers et al. 2009; Maloney et al., 2013) further refine the paleoseismic chronology of the West Tahoe Fault and show an event at about 4 thousand years before present. At Osgood Swamp, 500 m north of highway 50, Seitz (2015a; 2015b; Seitz and Mareschal, 2014; Seitz, 2014) conducted a paleoseismic investigation that included a fault trench. At this location the 3 m high fault scarp was found to be the result of three earthquakes that occurred during the past 10 ka. The C-14 dated stratigraphic section consisted of alluvial deposits overlying glacial till and outwash that was capped with peat layers and alluvium (Fig. 5).

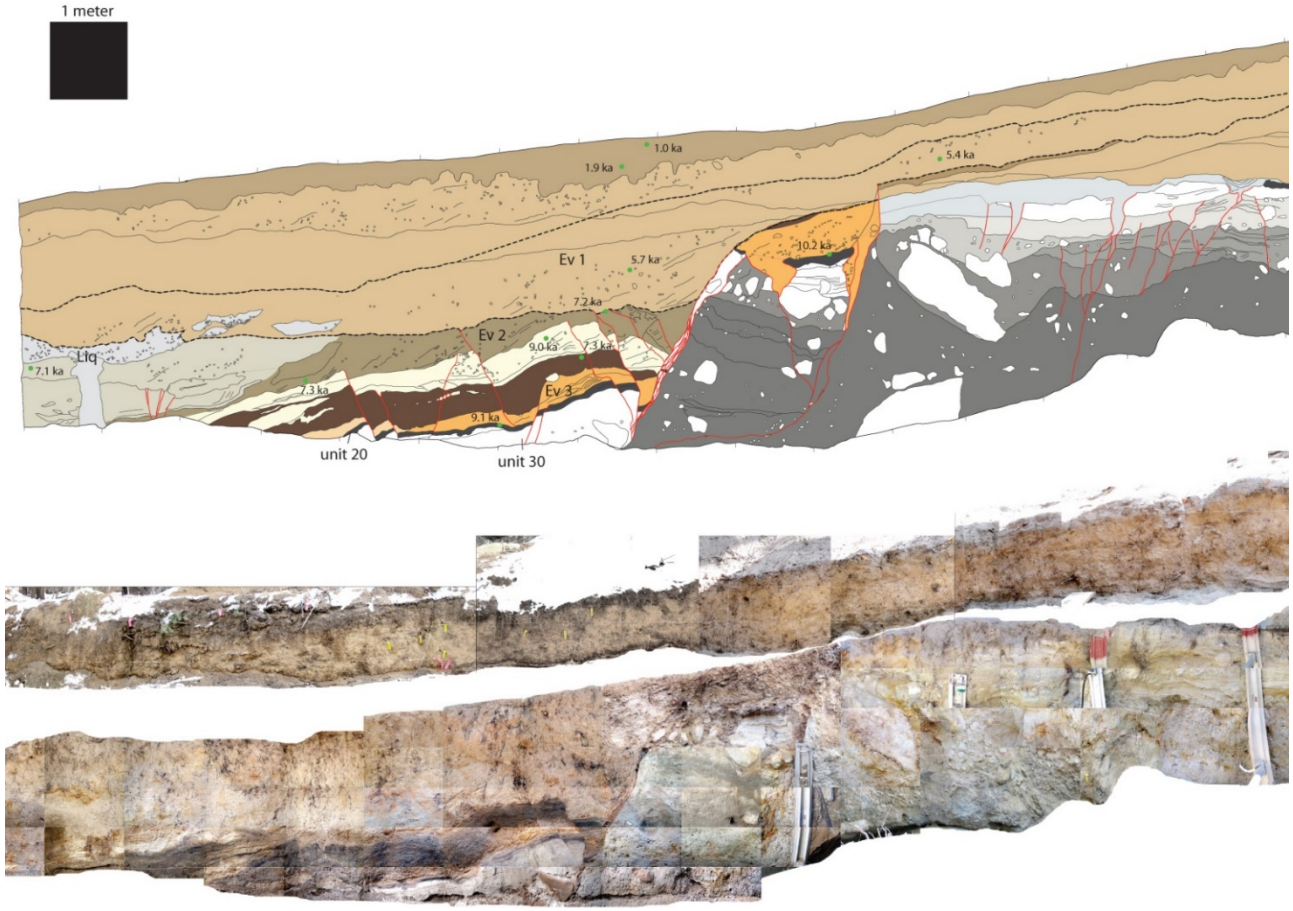

Figure 5. Fault Section 1 Trench Log. . Clear evidence for three earthquakes was identified during this 2013 USGS NEHRP funded project conducted by the California Geologic Survey (Seitz, 2015, Seitz and Mareschal, 2014). Radiocarbon dating confirms three events in the past 10 ka. The main fault is the sharp, left-sloping contact between gray glacial sediments and brown alluvial and scarp-derived colluvial sediments. The trench exposure is about 4 meters deep, image tiles are 1 meter horizontal by 0.5 meter vertical. The excavation was benched, the upper bench is the separate top mosaic and log. The top contact is the original ground surface. The surface soils and colluvium thicken on the left down-faulted block. Fault trench location is indicated in fig. 2, 6 and plate 2.

Previous Active Fault Maps

Following the multibeam bathymetric survey of Gardner et al. (1998; 2000) several active faults were mapped in Lake Tahoe. Some of these faults were previously recognized as active by Hyne et al. (1972) in their offshore study. Schweickert et al. (1999; 2000b) incorporated the offshore faults into a basin-wide mapping effort that included onshore extensions of these faults, and many more features interpreted as active faults. This work was summarized in the "Preliminary map of Pleistocene to Holocene faults in the Lake Tahoe Basin, California and Nevada" (Schweickert et al., 2000b). This map, as stated in their disclaimer, was a preliminary generalized map that was not intended to be used for planning purposes addressing seismic hazards. In practice, however, this caution was often ignored and the map was used for planning purposes. The detailed offshore studies based on seismic profiling and sediment cores (Kent et al., 2005; Dingler et al, 2009) have provided robust slip rate estimates. In contrast, the distribution and character of the onshore faults has been controversial (Bell et al., 2002; Kent et al., 2015; Dingler et al., 2009), and many features mapped as faults were later found to be non-tectonic geomorphic scarps or lineaments. Saucedo (2005) published an updated geologic map of the Tahoe Basin, which included an evaluation of mapped onshore faults from the Schweickert et al., (2000b) map. Peer review of the 2005 map, including group field reviews by geologists familiar with Lake Tahoe area geology, questioned the activity and the existence of onshore faults north of Emerald Bay, some of which were subsequently not included in the map by Saucedo (2005). Dingler et al. (2009) could not find evidence of faults that Schweickert et al. (2000; 2004) named the "Tahoe Sierra Frontal Fault" in Emerald Bay. More recent mapping by Howle et al. (2012) using a 2006 Lidar survey by the US Army Corps of Engineers (USACE) has reintroduced the Tahoe Sierra Frontal Fault as a zone of active faulting.

Evaluation of Previous Fault Maps

In general, availability of increasingly detailed and extensive Lidar surveys has increased our confidence in evaluating the geomorphology and origin of fault-like features. This study re-evaluated faults mapped by Howle et al. (2012) using the more recent Lidar survey by Watershed Sciences (2010). The Watershed Sciences Lidar survey used two Leica ALS50 Phase II laser systems mounted in a Cessna Caravan 208B. The Leica systems were set to acquire ≥ 83,000 - 105,900 laser pulses per second (i.e., 83 - 105.9 kHz pulse rate) and were flown at 900 - 1300 meters above ground level (AGL) depending on weather and terrain, capturing a scan angle of ±14° from nadir. These settings were developed to yield points with an average native pulse density of >8 pulses per square meter over terrestrial surfaces. The resulting average first-return density of delivered dataset is 11.82 points per square meter with an average ground point density of 2.26 points per square meter. The vertical accuracy was estimated at 3.5 cm RMSE. All the Tahoe Regional Planning Agency (TRPA) Lidar data is in the public domain and available at the OpenTopography website: (http://www.opentopography.org). Other factors that influenced our fault evaluation were field visits and the referenced offshore and basin-wide studies.

The single most important product allowing for more detailed mapping and more confidence in geomorphic interpretation is the bare earth Lidar digital elevation model (DEM). Survey points associated with the dense tree cover on the lower elevations of the basin can be removed so that the DEM depicts only the ground surface. The bare earth DEM was used to generate hill shade and slope shade images optimized for the recognition of fault scarps. Prior to the Watershed Sciences Lidar survey, the forest greatly obscured the thoroughgoing nature and relative sharpness of fault scarps.

Fault related geomorphic features are more distinct, continuous and recognizable in the higher resolution Lidar survey (Plate 2; Table 1). Fault features between Cascade and Fallen Leaf Lakes and south of Fallen Leaf Lake generally follow fault sections shown by Howle et al. (2012), but have been re-mapped as described below to take advantage of the new higher-resolution survey. Other sections near Emerald Bay and on-land north of Emerald Bay could not be verified as active faults. Features mapped by Howle et al. (2012) that could not be verified as active faults in this study can be interpreted as three broad categories of geomorphic features: 1) scarps in bedrock; 2) non-tectonic variations in glacial moraine crests and moraine slopes; and 3) landslide scarps. Geomorphic features corresponding to faults mapped by Howle et al. (2012) that are interpreted as not related to active faulting are shown on Plate 2. Additionally, copies of figures from Howle et al. (2012) are included with this report (Fig. 8, 9) for comparison of mapped faults with geomorphic features that have been interpreted from the higher-resolution Lidar survey.

Features interpreted by Howle et al. (2012) as active faults include several northwest trending aligned escarpments and linear drainages parallel to mapped bedrock faults (Features 22, 23, 26, and 33 on Plate 2). All of these features are developed in bedrock, and none are closely associated with scarps or other geomorphic features in Pleistocene glacial or alluvial deposits. Most of these features can be interpreted as due to differential erosion along bedrock faults. The scarps northwest of Emerald Bay (Feature 33 on Plate 2) appear to be relatively sharp up-slope facing scarps and graben. The topographic position of these features and their geometry suggests that they have formed by gravitational spreading of the ridge (as sackungen) rather than by faulting.

Several features, mapped as faults by Howle et al., (2012) are based on notches in the moraine crests. Two of these features were mapped on the Cascade Lake Tahoe-age left lateral moraine (Fig. 8). The first feature (37 on Plate 2) was mapped where two moraine crests merge, a depositional feature that resulted in erosion breaching the moraine and cutting a gully with associated levee deposition. This gully coincidently aligns with a fluvial cut (36) farther south. Lack of continuity of geomorphic features across an adjacent uniform-sloping Tioga-age maximum (~20 ka) moraine crest, and several additional crests, supports the interpretation that these features are not related to faulting. Similar features to the north (38 on Plate 2), probably have the same cause: merging moraines concentrated runoff, resulting in erosion and a gully down the moraine slope, in this case obscuring a portion of the Section 3 fault scarp near the

base of slope. Again, adjacent moraine crests show no displacement. Another similar feature (40 on Plate 2) on the northern end of the Emerald Bay Tioga-age right lateral moraine also appears to be glacial deposition and later erosion. In each of these cases, no consistent displacement on successive moraine crests or through-going scarps were observed to support an interpretation of active faulting.

North of Emerald Bay, Schweickert et al. (2004) and Howle et al. (2012) interpreted a series of scarps as evidence for active faulting. An image based on the Lidar (Howle et al. 2012, Fig. 8, 9) shows "scarps along base of over steepened range front." The more detailed Lidar survey of this area (Watershed Sciences, 2010), shows numerous, arcuate scarps suggesting landslide headscarps as well as some that can be interpreted as landslide toes (Features 45, 46, 47, and 50 on Plate 2). These features are distributed over a broad area, rather than forming narrow zones and sharply defined scarps, as found along the faults farther south. The general trend of these features suggests structural control of some scarps, either related to foliation and old bedrock faults or landslide scarps developed along bedrock zones of weakness. Although the trend of features extends south to Emerald Bay, the left lateral moraine crests there show no displacement. No displacement is observed in post Tioga-age lacustrine sediments in Emerald Bay (Kent et al., 2015; Brothers et al. 2011; Maloney et al., 2013). Howle et al. (2012) acknowledges that no sharp moraine crest scarps exist here and instead invoke extensional folding as the result of faulting at some depth. Considering the extensive Lidar coverage in the basin that clearly shows that these glacial deposits deform in a brittle scarp-forming fashion, no support for this interpretation could be found. The overall geomorphic expression of the features north of Emerald Bay is consistent with landsliding partially controlled by bedrock structure. The geomorphic expression of the Emerald Bay moraine crests as imaged by the new Lidar survey is not consistent with Holocene faulting. Therefore, evidence for active faulting in the northwest portion of the Emerald Bay Quadrangle as presented by Howle et al. (2012) is not convincing in light of the Watershed Sciences Lidar survey.

The extent of the Lidar survey used by Howle et al. (2012) does not include fault Section 1 described in the "fault geomorphology" below. Additionally, addressing the differences in active fault mapping, Kent et al. (2015) conducted a basin-wide fault evaluation that used the Watershed Sciences (2010) Lidar survey and the most comprehensive collection of offshore high-resolution seismic profiles. Kent et al. (2015) did not find evidence of active faulting onshore north of Emerald Bay.

Active Fault Geomorphology

West Tahoe Fault Sections

The West Tahoe Fault is described as 3 sections that are continuous, without major steps or trend changes within each section (Fig.2, Plates 1, 2). Sections, 1, 2, and 3 are 6 km, 12.2 km, and 5.5 km long, respectively. These fault sections exhibit an overlapping right-stepping pattern, with a 0.5 km step east from Section 1 to Section 2, and a 1 km step from Section 2 to Section 3. The northern portion of Section 3 trends offshore. North of Emerald Bay the uplifted shoreline is consistent with an offshore West Tahoe Fault accommodating the entire slip budget of the fault. This stepping pattern continues offshore along the mouth of McKinney Bay, where about 1 km further east the Stateline Fault trends approximately parallel to the West Tahoe Fault. Plate 2 is a fault map which includes an evaluation of geomorphic features that could be or have been interpreted by others to be active faults. All features are numbered and keyed to Table 1, which provides more details. The geomorphic features shown on Plate 2 are referred to in this text as stand-alone numbers in parentheses.

Fault Section 1

Fault Section 1 is the southernmost fault strand extending from Christmas Valley to Angora Lakes (Fig. 2, 6; Plates 1, 2). At the southern end of the fault, the fault scarp (4) does not extend across the flat valley floor, and several recessional moraines do not exhibit faulting (2). The linear valley margin, shown as a concealed fault by Saucedo (2005), is more likely due to glacial erosion (1).

To the north, the fault is located along the west side of the steep-sided glacial valley, alternating between the flat valley floor and glacial deposits. Because the glacial deposits may extend to considerable elevations above the valley, the fault climbs the valley slopes. The valleys have been dominantly shaped by glaciers and their deposits, and the movement on the West Tahoe fault has resulted only in a slight reshaping since the Pleistocene glaciations. From its southern end in Christmas Valley, the fault scarp climbs up the side of the valley slope northward towards Highway 50 (4, 6, 8; Plate 2). The east-facing scarp along this stretch is well defined in the Lidar imagery with scarp heights on the order of 1-3 m in Tioga-age glacial deposits and overlying alluvium. North of Highway 50, the fault is well expressed with a ~3 m high scarp in the left lateral Tioga-age moraine (9). Between the lateral moraines that surround the recessional moraine complex that includes Osgood Swamp, the east-facing fault scarp is less steep, with a height of 3 m (10, 11). In this area the fault scarp is less steep because the surface deposits include a thin layer of late Holocene sandy alluvium.

North of Osgood Swamp, a well-defined scarp in Tioga age till is continuous towards Angora Lakes (Fig. 6, Plate 2, Features: 12, 14, 16). The northern end of the fault between the upper and 2nd Angora Lake curves to the east towards the southern Fallen Leaf right lateral moraines.

Portions of the fault west of Osgood Swamp were mapped by McCaughey (2003). Our mapping along this section essentially overlaps Kent et al. (2015) and, in this area, the less detailed Howle et al. (2012) mapping. Howle et al. (2012) mapping was based on an earlier Lidar survey that did not extend this far south. The differences consist of the level of detail available and recognizable in the publications, and in the extent of individual fault strands.

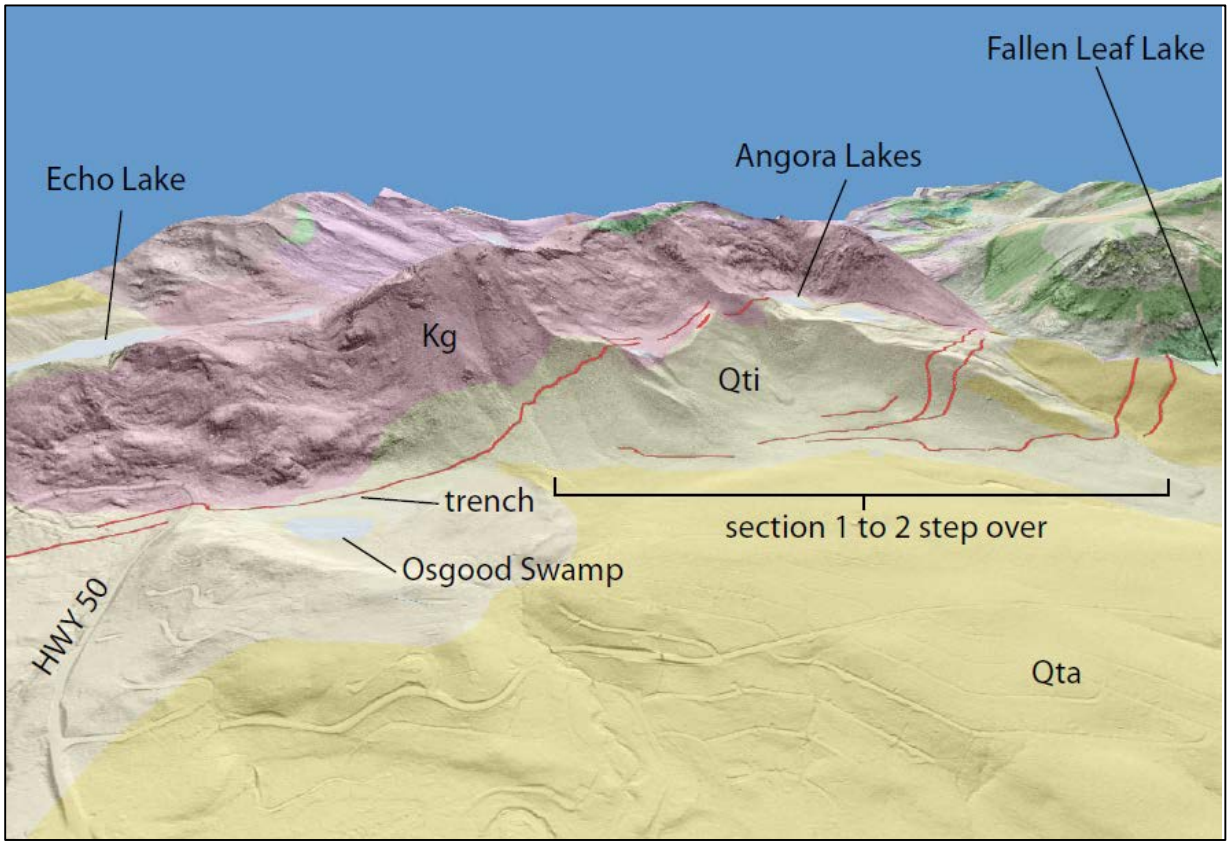

Figure 6. Oblique Lidar Hill Shade with Geologic Map and Faults from Highway 50 to Angora Lakes. Illustrates the fault climbing up the valley slopes in buttressed glacial deposits. Geology from Saucedo et al. (2005). The location of a paleoseismic investigation with trench is indicated (Seitz, 2015a; 2015b; Seitz and Mareschal, 2014).

Fault Section 1 to Section 2 Step-Over

North of the Osgood Swamp moraine complex, the Section 1 fault climbs up to Earthquake Lake (16; Kent et al., 2015) and continues to Angora Lakes (17). Here the fault takes a 500 m, nearly right angle turn down slope to the east, where the fault scarp nearly intersects the first prominent Section 2 fault scarp, which cuts across the extension of the Tahoe/Tioga–age moraine crests (Fig. 7). This fault bend matches the topography in that it runs along the base of the range front. Section 1 and Section 2 fault sections overlap by 1.7 km and an additional parallel branch fault exists further east. Overall this type of fault structure has been described as a step-over or relay

ramp structure with linkage (Faulds et al., 2011). All the faults in the step-over structure appear to have east-facing scarps. The western-most strands of this step-over have the sharpest scarps, which suggests greater recent activity and that the most recent surface rupture has been localized here, based on the continuity from the trench exposure at Osgood Swamp.

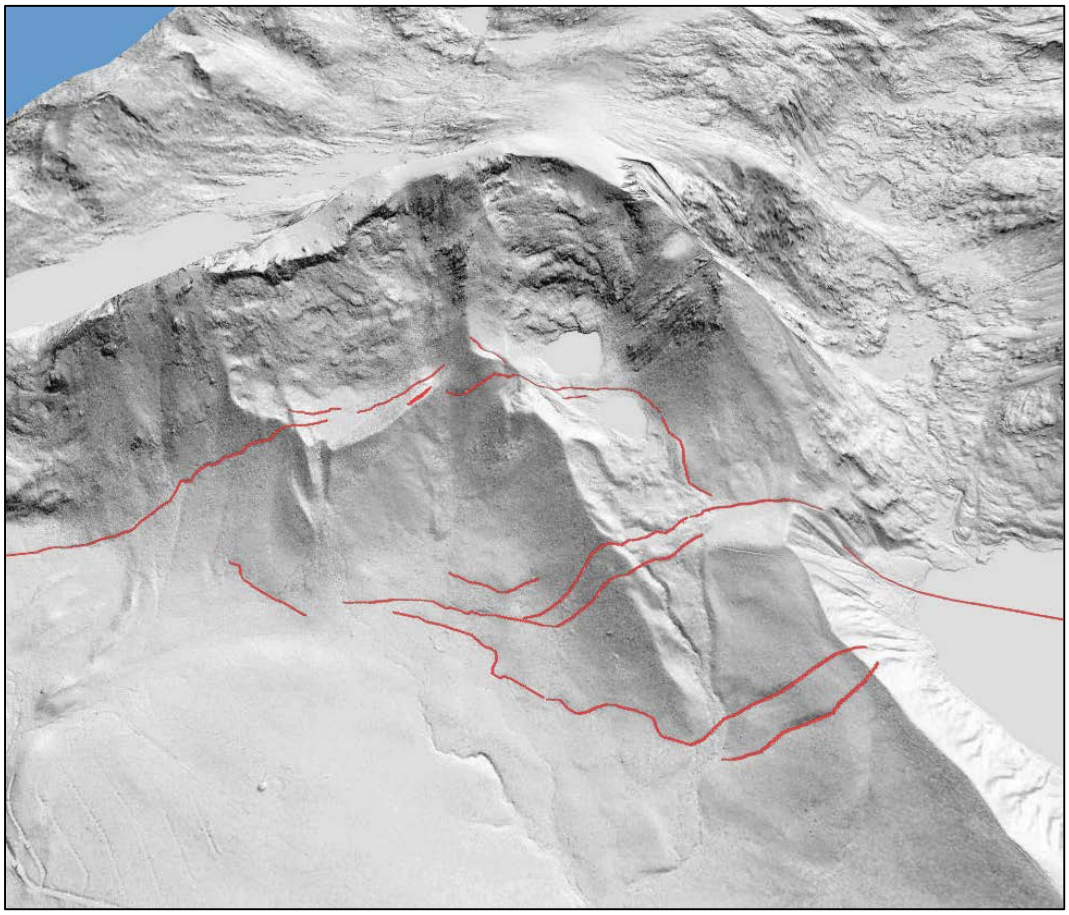

Figure 7. Oblique Lidar Hill Shade of the Fault Section 1 to Fault Section 2 Step-over Structure. Symmetrical fault lozenges are characteristic of these type of step over structures with fault linkages between the main fault strands.

Fault Section 2

Section 2 extends from north of the Osgood Swamp moraines to Emerald Bay**,** a length of 12.5 km (Fig. 2; Plates 1, 2). Where it branches from Section 1, it can be traced as a series of east-facing scarps that extend more northerly than Section 1**.** This section consists of sharp scarps in mostly Tioga-age glacial deposits (15). Within a notch with a flat valley trending northwest to southeast across the Tahoe and Tioga-age right lateral moraine has a clear down to the east scarp along the west side of this notch (19). The origin of this notch appears to be fluvial during the Tioga-age glacial period. There is no evidence for a west-dipping antithetic graben-forming

fault. Here the scarp is 3.8 m high (measured in this study with the 2010 Lidar survey, and 2008 Lidar survey by Howle et al., 2012), shows varying slopes, or is beveled indicative of multiple events, most likely a minimum of three, based on comparisons to the trench exposure at Osgood Swamp (Seitz, 2015a; 2015b; Seitz and Mareschal, 2014) and similar scarps at the northern end of Section 1 at Angora Lakes (17; Kent et al., 2015).

The east facing scarp in Tioga age deposits (19) can be traced north to the crest of the lateral moraine south of Fallen Leaf Lake. The north side of this moraine along the projection of the fault has been modified by numerous debris slide (20) and debris flow scars, removing any fault related features. Within Fallen Leaf Lake (21), the fault has been clearly observed in seismic profiles and multibeam bathymetry (Brothers et al., 2009; Maloney et al., 2013). Within the array of extensive seismic profiles the fault is expressed as a single strand with down to the east displacement. Maintaining its trend, the fault emerges on the northwest side of Fallen Leaf Lake with a clear scarp expressed as a steepened slope on the lake side of the moraine (24). From the Fallen Leaf Lake left lateral moraine crest, the fault scarp is clearly expressed to Cascade Lake along the flank of Mount Tallac (27, 28). Along the flank of Mount Tallac, glacial deposits are buttressed relatively high, this, it seems, leads the fault to daylight similarly high along the slope, following a similar pattern as observed along Section 1.

In Cascade Lake two fault strands (30) are observed in seismic profiles (Maloney et al., 2014) slightly to the east of the onshore projection. Geomorphically, the fault is much less well expressed on the north side of Cascade Lake over the moraine crest towards Emerald Bay. A reported bedrock shear (Howle et. al., 2012) along the range front visible in the highway 89 road cut dropping down to Emerald Bay with no clear Quaternary-age faulting may represent an active strand or a no longer active bedrock shear (31). From the north shore of Cascade Lake to Emerald Bay the fault is inferred.

Fault Section 3

This fault section is comprised of a parallel strand 1.5 km east of fault Section 2, 0.7 km northwest of the northwest end of Fallen Leaf Lake (Plate 2). This fault scarp has an onshore extent of 2.8 km, and may extend over 5 km offshore. It overlaps with Section 2 a minimum of 2.8 km and a maximum of 4.5 km. Onshore, the fault consists of a well-defined scarp in Tioga- and Tahoe-age glacial deposits. A remarkable series of recessional moraines is preserved along the north side of Fallen Leaf Lake. These recessional moraine crests range in age from the outermost, at the greatest distance east of Fallen Leaf Lake, Tioga maximum age of about 20 ka (Howle, et al., 2005; 2012), to about 10-12 ka, in Fallen Leaf Lake (Seitz and Mareschal, 2014; Seitz, 2015b). A series of these youngest moraines adjacent to Fallen Leaf Lake are not cut by this fault, and no fault was recognized in the high resolution seismic CHIRP profiles along this trend in Fallen Leaf Lake to the south (Kent et al., 2015; Brothers et al., 2009; Maloney et al., 2013). Scarp heights along this fault are about 3 m in Tioga-age deposits, increasing to about 10

m in Tahoe age deposits where the fault extends offshore adjacent to the right lateral Cascade Lake moraine. Dingler et al. (2009) describes an offshore side slope bench with pock marks that was interpreted as the possible existence of an active fault roughly along trend with this fault offshore to the north (39). This fault strand may represent a likely connecting structure to the most active portion of the West Tahoe Fault which lies offshore along the western base of Lake Tahoe.

Subsurface Investigation

In October 2013, Seitz (2015a; 2015b; Seitz and Mareschal, 2014; Seitz, 2014) conducted the first trenching study of the West Tahoe Fault (10). A site with fine-grained surface sediments was selected, as opposed to the boulder-rich moraine sediments that cover most of the onshore fault. At the trench site a 1.5 m surface layer of post-glacial sandy alluvium has resulted in a less steep scarp. However, the fault scarp continuity allows a confident recognition of fault displacement. In the bare earth Lidar images scarps are recognized as sharp slopes, generally over distances of less than 15 m.

The site is located ~3.5 km from the southern end of the mapped fault, adjacent to Osgood Swamp (Fig. 2, 6; Plate 2). The trench site is located within a morainal complex between prominent lateral moraines and upslope of a series of Tioga-age recessional moraines. The glacier originated from the Echo Lake valley to the west and flowed over the range crest eroding a prominent U-shaped notch in the ridge before flowing down 300 m to the flat valley floor. The excavation revealed an east-dipping, normal fault juxtaposing glacial deposits against datable peat-bearing and charcoal-rich younger alluvial sediments (Fig. 5). The glacial deposits and peat layers were matched across the fault. Clear evidence for three earthquakes is based on scarp-derived colluvium, fissures, faulted scarp-related alluvium, liquefaction, and upward terminations of faults. Retrodeformation of the faulted sediments results in co-seismic vertical displacements estimates of 1.4 m, 0.8 m and 1 m from the most recent to oldest event, respectively. Results from multiple C-14 analysis place the most recent event at ~5.5 ka, the penultimate event at ~7.2 ka, and the oldest event at ~9 ka. These events (Seitz, 2015a; 2015b; Seitz and Mareschal, 2014) appear to correlate well with earthquake event ages interpreted from offshore Lake Tahoe turbidites (Smith et al., 2013), and landslides in Fallen Leaf Lake (Maloney et al., 2013).

Fault Zone Width

Surface faulting investigation zones in California are traditionally 1000 feet wide. There are two issues that bear on the width of the zone of investigation: 1) what is the location of the primary fault; 2) what is the extent of secondary faulting. On strike-slip faults these zones are centered on the primary fault. On dip-slip faults the surface deformation is asymmetrical with a

significantly wider zone of deformation on the hanging wall. On normal faults, on the downthrown fault block it is common for parallel antithetic graben-forming faults to form in varying distances from the primary fault. Because sediment deposition is enhanced on the downthrown block, these secondary faults are often buried and not apparent in the geomorphology. In contrast, sedimentation on the upthrown block is less, and often decreased by the faulting. Secondary faulting uphill from the crest is relatively rare. To account for the wider zone of deformation on the downthrown block, Earthquake Fault Zones (EFZ) for the WTF are asymmetrical around the primary fault traces. The width ratio of these zones was informed by an empirical study of the Wasatch Fault (McCalpin, 1987), which reviewed 40 fault trench studies and concluded the mean horizontal distances of secondary faulting from the main faults were 1.8 m and 12.7 m on the upthrown and downthrown blocks, respectively. Previously, the USGS (Sharp, 1976) recommended asymmetrical investigation zone widths for the normal Wasatch fault. The Utah Geological Survey (2015) recommends widths of special study zones for normal faults of 500 ft and 250 ft, for the downthrown and upthrown sides of the fault, respectively. Based on these references, and consideration of the usual practice of delineating EFZ with 500 ft on either side of the primary fault traces, the EFZ for the West Tahoe Fault was delineated with roughly 400 ft on the upthrown block (west side) and roughly 600 ft on the downthrown side.

Faults Recommended for Zoning

There is clear evidence that the discussed onshore portion of the West Tahoe Fault is active with multiple events in the Holocene and poses a surface rupture hazard. Although the main strain markers are glacial landforms and deposits that may be older than 11 ka, the strong event evidence from on-fault studies combined with the high-resolution Lidar imagery that indicates fault continuity, allows a confident surface rupture hazard assessment.

Fault sections 1, 2 and 3 shown in Fig. 2 and Plate 1, 2 are deemed sufficiently active and well defined and are recommended for surface rupture hazard zoning. The faults shown on Plate 3 are recommended to be zoned with 600/400 ft width on the downthrown and upthrown blocks respectively.

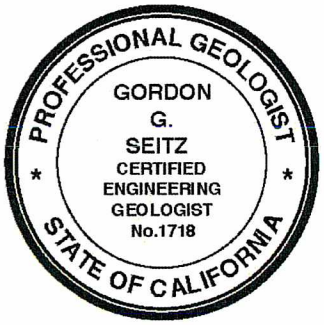

Gordon G. Seitz
Engineering Geologist
PG 5514, CEG 1718
November 16, 2015

reviewed recommendations approved
Chris J. Wills

Table 1 Tectonic and Non-Tectonic Geomorphic Features. Numbered features shown on Plate 2 on a Lidar Hill Shade base.

Feature	Description
1	linear margin of valley, west side: result of infilling of a U-shaped glacial valley, no indication of tectonic origin, no oversteepening of slope as observed elsewhere along the WTF immediately to the north.
2	arc-shaped recessional moraines, continuous except for breaks related to fluvial incision.
3	linear slope bench, appears to be part of a recessional moraine, possibly a resistant bedrock unit as indicated by slope outcrops to the south.
4	well-defined east-facing scarp, oversteepened slope in Qti.
5	linear margin of valley, west side: result of infilling of a U-shaped glacial valley, no indication of tectonic origin, no oversteepening of slope as observed elsewhere along the WTF to the south and north, lateral Qti moraines along a northward projection are continuous and unfaulted.
6	well-defined east-facing scarps in Qti moraines
7	artificial cut (quarry) at the terminus of Qti lateral moraine.
8	well-defined east-facing scarp in latest Qti, correlations with fault in trench (10). consistent with faulting younger than ~10ka.
9	well-defined east-facing scarp in Qti lateral moraines, vertical displacement ~3m.
10	Fault trench location. The trench crossed a well-defined east-facing 3 m high scarp in Qti covered by a thin layer of alluvium. Three events were recognized in the past 10 ka (Seitz, 2014, Seitz and Mareschal, 2014, Seitz, 2015a,b)
11	sag pond along fault, minor antithetic graben-forming faults may exist.
12	well-defined 4+ m high scarp in Qti lateral moraines, deposits here are older than the faulted units exposed at the trench site location 10.
13	west-facing fluvial scarp in Qta.
14	well-defined scarp expressed as an over-steepened slope in Qti.

Feature	Description
15	east-facing scarps in Qti ranging in heights from 0.5 m to 1 m, inferred to be faults. The pattern of faulting is consistent with faults linking fault step-overs.
16	east-facing scarps in Qti and younger pond deposits, described as Earthquake Lake in Kent et al. (2015).
17	well defined scarp in Qti moraines, multiple events are suggested by scarp bevel (Kent et al., 2015)
18	moderately defined east-facing scarps in Qta, most likely 70-130 ka, possibly an older glaciation, inferred as active faults. These structures are consistent with linkage faults of a step-over structure from Section 1 to Section 2.
19	well-defined east-facing scarp in Qti, beveled scarp face suggests multiple events consistent with the trench fault investigation (10) to the south, and offshore paleoseismic study to the north (21).
20	recent landslide scar. The ridge at the top of the slide is a remnant of the head scarp and not a moraine crest, hence it is much younger and may not exhibit fault displacements. Deposits consistent with this slide location are evident in the offshore data (21).
21	The fault clearly displaces latest Holocene-age lacustrine sediments as well documented in seismic profiles and multibeam bathymetry combined with C-14 dated sediment cores (Brothers et al., 2011, Maloney et al., 2014).
22	steps in jointed bedrock have been mapped by Howle et al.(2012) as Quaternary-age faults. No evidence for Holocene activity is observed.
23	A lineament in jointed bedrock has been mapped by Howle et al. (2012) as a Quaternary-age fault. This feature is exaggerated by the coincidental alignment with an erosional gully. No evidence for Holocene activity is observed.
24	well-defined scarp on left-lateral Qti moraine, observed as an over-steepened slope. Very difficult to observe in the field, yet clear in the slope shade or optimally oriented hill shade.
25	moderately defined east-facing scarps in Qta(?) glacial till These scarps are somewhat suspect as they parallel the glacial depositional direction, yet their sharpness suggests recent faulting. These features are inferred to be faults.

Feature	Description
26	Loomis (1981), Reid (1989) and Saucedo (2005) mapped a bedrock (Jurrasic-age) fault along this lineament with a west-side-down, right-lateral motion. Howle et al. (2012) shows this fault as a Quaternary fault. This feature is largely located on the steep east face of Mount Tallac where differential erosion has resulted in prominent east-facing cliffs. The sense of displacement does not match the observed active faulting and no evidence for Holocene faulting activity is observed.
27	well-defined scarps in Qti till at Tallac Creek reported in Kent el.,(2015) and Howle et al. (2012).
28	well-defined scarp in Tioga-age till, similar-aged talus and colluvium. Howle et al. (2012) has mapped additional strands branching to the north parallel to the near vertical foliation in granitic bedrock (Saucedo, 2005). We interpret these features to be the result of differential erosion.
29	well-defined scarp on the left lateral Qti moraine inner slope extending to Cascade Lake.
30	Two fault strands in Tioga-aged lacustrine sediments are observed in seismic profiles reported by Maloney et al. (2013).
31	The fault is poorly defined north of Cascade Lake. It is inferred based on a notch in the Qti moraine crests that may also be the result of other glacial or fluvial processes. The fault is inferred from the crest to Emerald Bay. A bedrock shear reported by Howle et. al., (2012) is visible in the Highway 89 road cut near Emerald Bay may represent an active strand or a no longer active bedrock shear.
32	Scarp in bathymetry was interpreted by Howle et al. (2012) as an active fault. Maloney et al. (2013) used seismic profiles combined with bathymetry to conclude that a faulting origin cannot be excluded. We infer the existence of a possible fault here, which may be consistent with linkage faults in a step-over, but also recognize other possibilities.
33	A lineament in jointed bedrock has been mapped by Howle et al. (2012) as a Quaternary-age fault. This feature is characterized by scarps that appear to form a graben, which is consistent with this feature being a sackung. The bedrock foliation is steep and parallel to this feature. No clear evidence for Holocene faulting activity is observed. Note: prominent bedrock joints in Kg (Saucedo, 2005), 3 km to the northwest for comparison.
34	series of continuous recessional moraines. These are located along the southward trend of the Section 3 fault strand. Seismic investigations farther south along this same trend in Fallen Leaf Lake did not find any faulting (Maloney et al., 2014).
35	well-defined east-facing scarp in Qti and Qta till.

Feature	Description
36	short linear east-facing scarp in Qta. Howle et al. (2012) shows this feature as a Quaternary active fault. This scarp is located at the terminus or nose of a moraine, the relative sharpness appears to be the result of fluvial modification. Lack of continuity across well-defined glacial landforms to the north and south suggests that this is not fault related.
37	gully on right-lateral moraine (Qta) slope, the result of the moraine crest being breeched by ponded water. The lower portion of the gully has experienced debris flow levee deposition. This feature was mapped as a Quaternary active fault by Howle et al. (2012) and continued to the north through Cascade Lake and Emerald Bay. The Qti moraine crest immediately to the north is continuous.
38	gully on right-lateral moraine (Qta) slope, the result of the moraine crest being breeched by ponded water. This gully has obscured the fault scarp as mapped by us. Howle et al. (2012) extended the fault from the south to this gully and northward across Emerald Bay. The Qti moraine crest to the north is continuous.
39	pock marks on offshore side slope. These are crater-like features that Dingler et al. (2009) describes as possibly the results of springs or degassing along a fault. These features are located along the offshore extension of the onshore fault.
40	gully on the south slope of the right-lateral moraine (Qti) of Emerald Bay. This gully has formed along a low of the moraine crest. Merging of crests focusing the flow of surface drainage and/or primary glacial deposition is interpreted to have formed this feature. Moraine crests to the north are continuous. Long profiles along the moraine crest are consistent with primary glacial deposition. Howle et al. (2012) interpreted this feature as a Quaternary active fault.
41	well-defined east-facing scarp in Qti till and across three moraine crests. This fault may extend into Emerald Bay, however it was not observed in a 3d seismic grid (Maloney et al. 2014) and the Emerald Bay right-lateral moraines do not exhibit faulting along this trend. To the north this fault trends offshore and may connect with the primary WTF (Dingler et al., 2009), though the primary strand may well be further east.
42	older generation of debris slides on Qti moraines, truncating the moraine crests.
43	debris flows on the south slope of the left-lateral Qti moraines , some postdating debris slides at 42.
44	inset alluvial/colluvial range front apron or debris cone between bedrock highs. The relatively low angle slope of the inset surface combined with a possible head scarp is also consistent with an old landslide at least pre Qti. The possible head scarp elevation matches the adjacent large slides to the north fairly well (45 and 49).

Feature	Description
45	well-defined large rotational slide scarps. Characteristic arcuate scarp with an inset down-dropped slide mass. Howle et al. (2012) indicates these scarps as:” scarps along base of over-steepened range front” and attributes them to active faults (Howle et al.2012; fig 5).
46	multiple smaller rotational slides within the larger slide mass.
47	debris flows
48	elevated shelf is consistent with an offshore West Tahoe Fault north of the Section 2 to Section 3 step over
49	well-defined large rotational slide scarps. Characteristic arcuate shaped scarp with an inset down-dropped slide mass. Howle et al. (2012) indicates these scarps as:” scarps along base of over-steepened range front” and attributes them to active faults (Howle et al.2012; fig 5). Our evaluation does not recognize any active faulting.
50	well-defined land slide toes.
51	Fig. 8, indicates the features we evaluated on Howle et al., (2012, Fig.4). Details: points 29-46.
52	Fig. 9, indicates the features we evaluated on Howle et al., (2012, Fig.5). Landslide scarps along this range front were interpreted by Howle et al. (2012) as active faults. Details: points: 33-50.

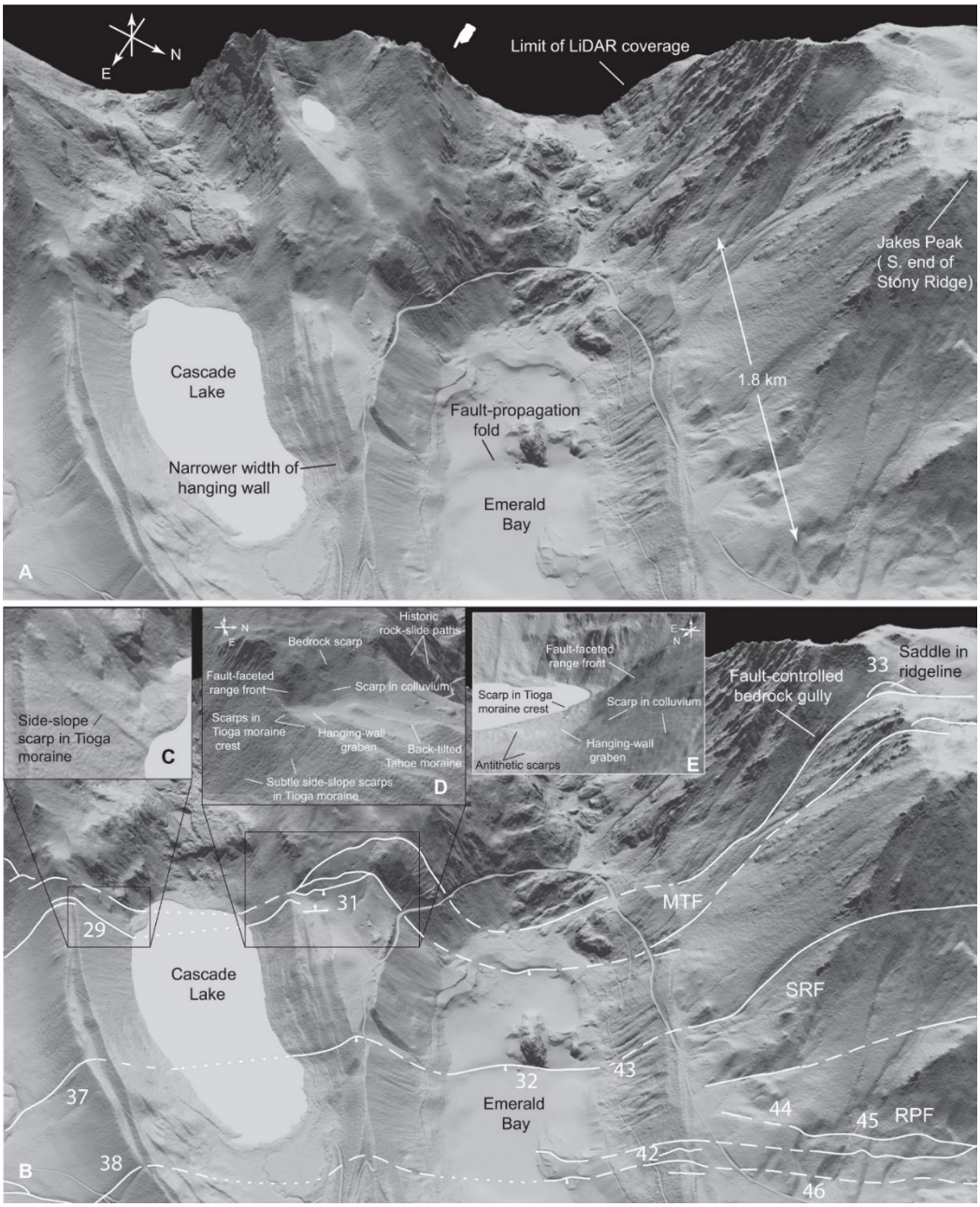

Figure 8. Oblique Bare-Earth Lidar Hill Shade Image Cascade Lake and Emerald Bay. This is Fig.4 from Howle et al. (2012), the bottom image (B) was modified with numbered features that we evaluated in Table 1.

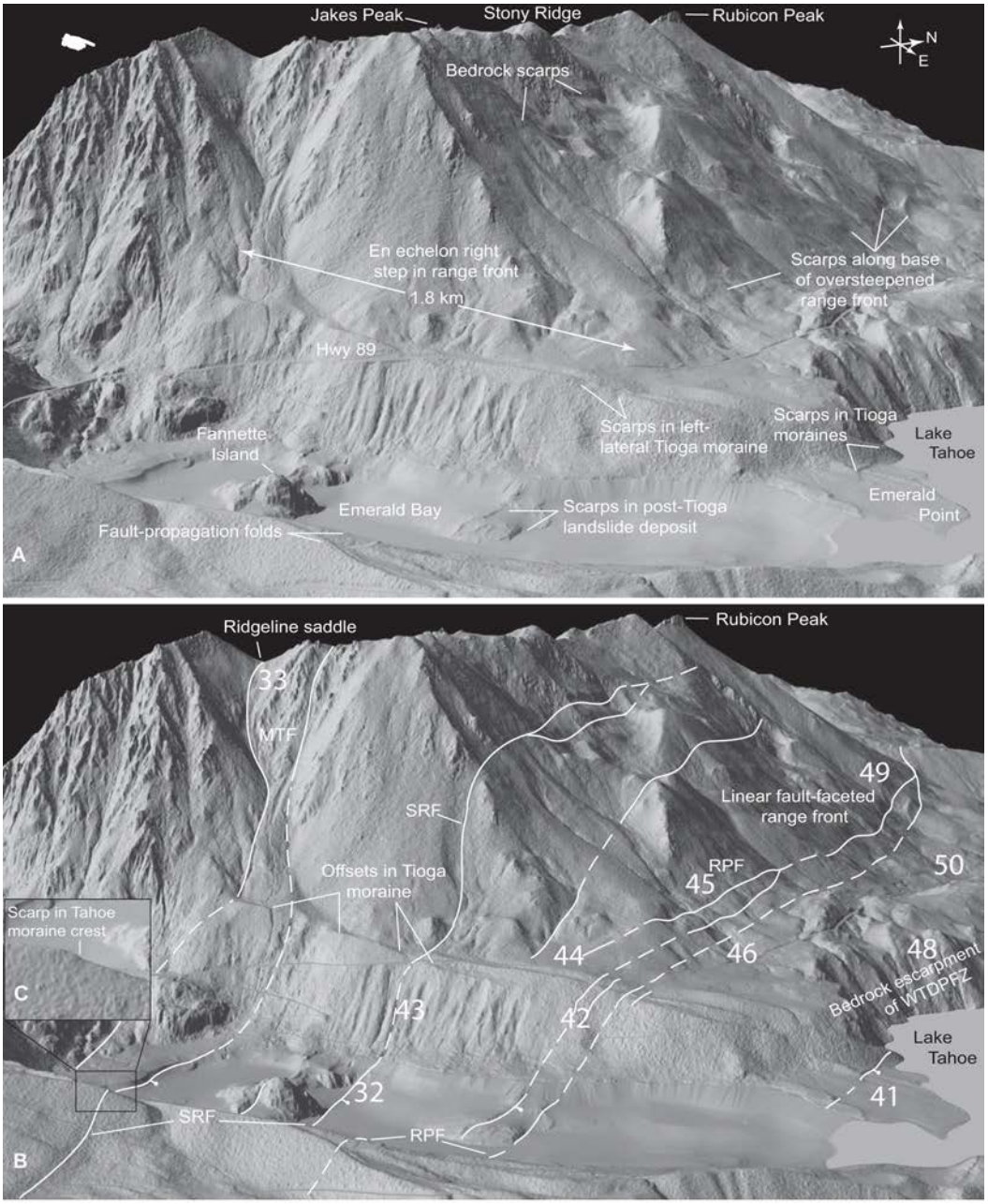

Figure 9. Oblique Bare-Earth Lidar Hill Shade Image North of Emerald Bay. The top and bottom are Fig. 5 from Howle et al. (2012), the bottom image (B) was modified with numbered features that we evaluated and describe in Table 1. Several of these slides were also shown on a map by Howle et al. (2012), data repository Fig. 2, but the landslide origin was apparently not accepted as the origin of the scarp. They linked landslide scarps to infer the existence of faults.

REFERENCES

Bell, J.W., Ramelli, A.R., Caskey, J.S., 2002, Uncertainties associated with active faults mapped in the Lake Tahoe Basin, AEG annual meeting in Reno, abst.

Birkeland, P.W., 1961, Pleistocene history of the Truckee area, north of Lake Tahoe, California: Stanford University, Ph.D. dissertation, 126 p., Plate 1, scale 1:62,500.

Birkeland, P.W., 1964, Pleistocene glaciation of the northern Sierra Nevada north of Lake Tahoe, California: Journal of Geology, v. 72, p. 810-825.

Blackwelder, E., 1931, Pleistocene glaciation in the Sierra Nevada and Basin Ranges: Geol. Soc. Amer. Bul, v.42, p 865-922.

Bormann, J. M., 2013, New Insights into Strain Accumulation and Release in the Central and Northern Walker Lane, Pacific-North American Plate Boundary, California and Nevada, USA [Doctorate Dissertation]: University of Nevada, Reno, 150 p.

Brothers, D. S., Kent, G. M., Driscoll, N. W., Smith, S. B., Karlin, R., Dingler, J. A., Harding, A. J., Seitz, G. G., and Babcock, J. M., 2009, New constraints on deformation, slip rate, and timing of the most recent earthquake on the West Tahoe-Dollar Point Fault, Lake Tahoe Basin, California: Bulletin of the Seismological Society of America, v. 99, no. 2A, p. 499-519.

Bryant, W.A., and Hart, E.W., 2007, Fault-rupture hazard zones in California: California Geological Survey Special Publication 42, p.42.

Burnett, J.L., 1982, Geologic map of Lake Tahoe: California Division of Mines and Geology, unpublished mapping, scale 1:62,500.

Dingler, J., Kent, G., Driscoll, N., Babcock, J., Harding, A., Seitz, G., Karlin, B., and Goldman, C., 2009, A high-resolution seismic CHIRP investigation of active normal faulting across Lake Tahoe Basin, California-Nevada: Geological Society of America Bulletin, v. 121, no. 7-8, p. 1089-1107.

Faulds, J.E., Henry, C.D., and Hinz, N.H., 2005, Kinematics of the northern Walker Lane: An incipient transform fault along the Pacific-North American plate boundary, Geology v. 33, p. 505-508.

Faulds, J.E., Hinz, N.H., Coolbaugh, M.F., Cashman, P.H., Kratt, C., Dering, G., Edwards, J., Mayhew, B., McLachlan, H., 2011, Assessment of Favorable Structural Settings of Geothermal Systems in the Great Basin, Western USA, In: Transactions. GRC Annual

Meeting; 2011/10/23; San Diego, CA. Davis, CA: Geothermal Resources Council; p. 777–783.

Fisher, G.R., 1989, Geologic map of the Mount Tallac roof pendant, El Dorado County, California: U.S. Geological Survey Miscellaneous Field Studies Map MF-1943, scale 1:24,000.

Gardner, J.V., Mayer, L.A. and Hughes-Clarke, J.E., 1998, The bathymetry of Lake Tahoe, California-Nevada: U.S. Geological Survey Open-File Report OF 98-509.

Gardner, J.V., Mayer, L.A. and Hughes-Clarke, J.E., 2000, Morphology and processes in Lake Tahoe (California-Nevada): Geological Society of America Bulletin, v. 112, n. 5, p. 736-746.

Hammond, W.C., and Thatcher, W., 2004, Contemporary tectonic deformation of the Basin and Range Province, western United States; 10 years of observation with the Global Positioning System: Journal of Geophysical Research, v. 109, no. B8, doi:10.1029/2003JB002746.

Howle, J.F., Finkel, R.C., Seitz, G., 2005, Cosmogenic exposure ages for Tioga and Tahoe age moraines at Meeks Bay, Lake Tahoe, California, Geol. Soc. Amer. Annual mtg. abst.

Howle, J. F., G. W. Bawden, R. A. Schweickert, R. C. Finkel, L. E. Hunter, R. S. Rose and B. von Twistern, 2012, Airborne LiDAR analysis and geochronology of faulted glacial moraines in the Tahoe Sierra frontal fault zone reveal substantial seismic hazards in the Lake Tahoe region, California-Nevada, USA, Bull. Geol. Soc. Am., doi. 10.1130/830598.1

Hyne, N. J., Chelminski, P., Court, J. E., Gorsline, D. S., and Goldman, C. R., 1972, Quaternary History of Lake Tahoe, California-Nevada: Geological Society of America Bulletin, v. 83, no. 5, p. 1435-1448.

Ichinose, G.A., Anderson, J.G., Satake, Kenji, Schweickert, R.A. and Lahren, M.M., 2000, The potential hazard from tsunami and seiche waves generated by large earthquakes within Lake Tahoe, California-Nevada: Geophysical Research Letters, v. 27, no. 8, p. 1203-1206.

Karlin, R.E., Schweickert, R., Lahren, M., Shane, S., Patterson, M., Dinkelman, I. and Seitz, G., 2001, Late Quaternary history of landsliding and faulting in Lake Tahoe: Geological Society of America Abstracts with Programs, v. 33 n. 3, p. 71.

Kent, G. M., Babcock, J. M., Driscoll, N. W., Harding, A. J., Dingler, J. A., Seitz, G. G., Gardner, J.V., Mayer, L. A., Goldman, C. R., Heyvaert, A. C., Richards, R. C., Karlin, R.,

Morgan, C.W., Gayes, P.T., and Owen, L.A., 2005, 60 k.y. record of extension across the western boundary of the Basin and Range province: Estimate of slip rates from offset shoreline terraces and a catastrophic slide beneath Lake Tahoe: Geology, v. 33, no. 5, p. 365-368.

Kent, G, Schmauder, G, Maloney, J., Driscoll, N., Kell, A.M., Smith, K., Baskin, R., Seitz, G., 2015, Reevaluating late Pleistocene and Holocene active faults in the Tahoe Basin, California-Nevada, AEG special pub.

Loomis, A.A., 1983, Geology of the Fallen Leaf Lake 15' quadrangle, El Dorado County, California: California Division of Mines and Geology Map Sheet 32, scale 1:62,500.

Maloney, J.M., Noble, P.J., Driscoll, N.W., Kent G.M., Smith, S.B., Schmauder, G.C., Babcock, J.M., Baskin, R.L., Karlin, R., Kell, A.M., Seitz, G.G., Kleppe, J.A., 2013, Paleoseismic history of the Fallen Leaf Segment of the West Tahoe-Dollar Point fault reconstructed from slide deposits in the Lake Tahoe Basin, California-Nevada, Geosphere, v. 9, no. 4, p. 1065-1090. doi: 10.1130/GES00877.1.

McCalpin, J.P., 1987, Recommended setback distances from active normal faults, Selected Works Utah State University, http://works.bepress.com/james_mccalpin/7

McCaughey, J.W., 2003, Pleistocene glaciation of the southwest Tahoe Basin, Sierra Nevada, California: University of Nevada, Reno, M.S. thesis, 179 p., Plate 1, scale 1:15,400.

Saucedo, G. J., 2005, Geologic map of the Lake Tahoe Basin, California and Nevada: California Geological Survey, Regional Geologic Map No. 4, scale 1:100,000.

Sharp, V.J., 1976, Earthquake hazard reduction in Utah; A report to the 42nd Utah State Legislature Research, Report No. 14, Dec., 1976, p. 1-56.

Schweickert, R. A., Lahren, M. M., Smith, K., and Karlin, R., 1999, Preliminary fault map of the Lake Tahoe Basin, California and Nevada: Seis. Res. Lett., v. 70, p. 306-312.

Schweickert, R.A., Lahren, M.M., Karlin, R.E., Smith, K.D. and Howle, J.F., 2000b, Preliminary map of Pleistocene to Holocene faults in the Lake Tahoe Basin, California and Nevada: Nevada Bureau of Mines and Geology Open-File Report 2000-4, scale 1:100,000.

Schweickert, R.A., Lahren, M.M., Karlin, R., Howle, J. and Smith, K., 2000a, Lake Tahoe active faults, landslides, and tsunamis, in Lageson, D.R., Peters, S.G. and Lahren, M.M., editors, Great Basin and Sierra Nevada: Geological Society of America Field Guide 2, p. 1-22.

Schweickert, R. A., Lahren, M. M., Smith, K. D., Howle, J. F., and Ichinose, G. A., 2004,

Transtensional deformation in the Lake Tahoe region, California and Nevada, USA: Tectonophysics, v. 392, no. 1-4, p. 303-323.

Seitz, G., and Kent, G, 2004, Closing the gap between on and offshore paleoseismic records in the Lake Tahoe Basin, NEHRP external tech report, 04HQGR007.

Seitz, G. and Mareschal, M., 2014, Multiple-Event Deformation on the West Tahoe Fault from Lidar and Trenching: Reconciling On and Offshore Paleoseismology, American Geophysical Union, Fall Meeting 2014, abstract #T41C-4666.

Seitz, G. 2015a, Tahoe Basin Fault Behavior from Integration of On and Offshore Paleoseismology, Basin and Range Province Seismic Hazards Summit III, Salt Lake City, Utah Geological Survey publications, p.1-4.

Seitz, G. 2015b, Characterization of the Highest Slip Rate Fault in the Lake Tahoe Basin: Paleoseismic Investigation of the West Tahoe Fault, USGS NEHRP technical report Intermountain West.

Seitz, G.G., 2014, Seismic Hazard Investigation of Lake Tahoe Using New Remote Operated Submarine: Dive Test in Support of Antarctic Subglacial Research (WISSARD) Project, Alfred E. Alquist Seismic Safety Commission, California Seismic Safety Commission Publication 2014-02.

Smith, S.B., Karlin, R.E., Kent, G., Seitz, G., and Driscoll, N.W., 2013, Holocene subaqueous paleoseismology of Lake Tahoe: Geological Society of America Bulletin, v. 125, p. 691–708, doi:10.1130/B30629.1.

Surpless, B.E., Stockli, D.F., Dumitru, T.A., and Miller, E.L., 2002, Two –phase westward encroachment of Basin and Range extension into the northern Sierra Nevada, Tectonics v.21, 1002.

UGS, (in prep.), Guidelines for evaluating surface-fault rupture hazards in Utah, 2nd edition.

Unruh, J., Humphrey, J., and Barron, A., 2003, Transtensional model for the Sierra Nevada frontal fault system, eastern California: Geology, v. 31, no. 4, p. 327-330.

Wells, D., and Coppersmith, K.J., 1994, New empirical relationships among magnitude, rupture length, rupture width, rupture area, and surface displacement: Bul. Seis. Amer., v.84, p. 974-1002.

Watershed Sciences, 2010, LiDAR Remote Sensing, Lake Tahoe Watershed, prepared for the Tahoe Regional Planning Agency, January 31, 2011.